BULLETIN OF THE POLISH ACADEMY OF SCIENCES
TECHNICAL SCIENCES
Vol. 55, No. 2, 2007

Invited paper

Nano-mechanics or how to extend continuum mechanics to nano-scale

J. WANG[1], B.L. KARIHALOO[2*], and H.L. DUAN[2]

[1]LTCS and Department of Mechanics and Engineering Science, Peking University, Beijing, 100871, P. R. China
[2]School of Engineering, Cardiff University, Queen's Buildings, The Parade, Cardiff CF24 3AA, UK

Abstract. In a series of recent papers we have shown how the continuum mechanics can be extended to nano-scale by supplementing the equations of elasticity for the bulk material with the generalised Young-Laplace equations of surface elasticity. This review paper begins with the generalised Young-Laplace equations. It then generalises the classical Eshelby formalism to nano-inhomogeneities; the Eshelby tensor now depends on the size of the inhomogeneity and the location of the material point in it. The generalized Eshelby formalism for nano-inhomogeneities is then used to calculate the strain fields in quantum dot (QD) structures. This is followed by generalisation of the micro-mechanical framework for determining the effective elastic properties of heterogeneous solids containing nano-inhomogeneities. It is shown that the elastic constants of nanochannel-array materials with a large surface area can be made to exceed those of the non-porous matrices through pore surface modification or coating. Finally, the scaling laws governing the properties of nano-structured materials are given.

Key words: surface/interface stress, generalized Young-Laplace equation, Eshelby formalism, effective elastic constants, size effect, scaling laws.

1. Introduction

For nano-structured [1] and nanochannel-array materials [2,3] with a large ratio of the surface/interface to the bulk, the surface/interface stress effect can be substantial. Thus, materials such as thin films, nanowires and nanotubes may exhibit exceptional properties not noticed at the macro-scale. As small devices and nanostructures are all pervasive, and the elastic constants of materials are a fundamental physical property, it is important to understand and predict the size-effect in mechanical properties of materials at the nano-scale. Many attempts have been made recently to reveal the influence of surface elasticity on the elastic properties of nanobeams, nanowires, nanoplates, and the results showed that the elastic moduli of monolithic and heterogeneous materials vary with their characteristic size due to the surface stress effect [4–9].

In this paper, we shall summarize the recent results of the authors on the surface/interface stress effects on the mechanics of nano-heterogeneous materials. These results include the Eshelby formalism for spherical nano-inhomogeneities and its application, the fundamental micromechanical framework for the prediction of the effective elastic moduli of heterogeneous materials, and the novel effective elastic constants of nanochannel-array materials obtained by manipulation of their surface properties. Moreover, the scaling laws governing the properties of nano-structured materials are given.

2. Eshelby formalism with surface/interface stress effects

2.1. Basic equations. The basic equations for solving boundary-value problems of elasticity consist of the following conventional equilibrium equations, constitutive equations, and strain-displacement relations for the matrix and the inhomogeneity:

$$\nabla \cdot \boldsymbol{\sigma}^k = 0\,,\ \boldsymbol{\sigma}^k = \mathbf{C}^k : \boldsymbol{\varepsilon}^k,\ \boldsymbol{\varepsilon}^k = \frac{1}{2}\left(\nabla \otimes \mathbf{u}^k + \mathbf{u}^k \otimes \nabla\right) \tag{1}$$

where $\boldsymbol{\sigma}^k$, $\mathbf{u}^k$ and $\boldsymbol{\varepsilon}^k$ denote the stresses, displacements and strains in Ω_I (inhomogeneity) and Ω_m (matrix), respectively. $\mathbf{C}^k$ are the elastic moduli of Ω_I and Ω_m. In what follows, as we will study both spherical inhomogeneities and cylindrical fibres, we will use the super- and sub-script $k = p$ for the former, $k = f$ for the latter, with $k = m$ denoting the matrix. Equations (1) have to be supplemented by the surface/interface elasticity equations to complete the mathematical description of the problem.

Surface/interface stress can be defined in various ways, for example, the surface/interface excess of bulk stress [10]. An extra group of basic equations is needed in addition to those of classical elasticity. To derive these, consider a system consisting of two solids Ω_I and Ω_m with different material properties. By considering the equilibrium of a general curved interface Γ with unit normal vector $\mathbf{n}$ between the two materials Ω_I and Ω_m (in subsequent Sections, Ω_I and Ω_m will denote an inhomogeneity

*e-mail: karihaloob@cf.ac.uk

and matrix, respectively), the equilibrium equations of the interface can be obtained [11,12]

$$[\boldsymbol{\sigma}] \cdot \mathbf{n} = -\nabla_S \cdot \boldsymbol{\tau} \tag{2}$$

where $[\boldsymbol{\sigma}] = \boldsymbol{\sigma}^I - \boldsymbol{\sigma}^m$, $\boldsymbol{\sigma}^I$ and $\boldsymbol{\sigma}^m$ are the volume stress tensors in Ω_I and Ω_m, respectively, $\nabla_S \cdot \boldsymbol{\tau}$ denotes the interface divergence of the interface stress tensor $\boldsymbol{\tau}$ at Γ [11]. Equation (2) is the generalized Young-Laplace equation for solids. It can be derived in various ways, for example, by the principle of virtual work. For a curved interface Γ with two orthogonal unit base vectors $\mathbf{e}_1$ and $\mathbf{e}_2$ in the tangent plane and a unit vector $\mathbf{n}$ perpendicular to the interface, $\nabla_S \cdot \boldsymbol{\tau}$ can be expressed as follows [7]:

$$\begin{aligned}\nabla_S \cdot \boldsymbol{\tau} = &\left(-\frac{\tau_{11}}{R_1} - \frac{\tau_{22}}{R_2}\right)\mathbf{n} + \frac{\mathbf{e}_1}{\mathrm{h_1 h_2}} \\ &\times \left[\frac{\partial(h_2\tau_{11})}{\partial\alpha_1} + \frac{\partial(h_1\tau_{21})}{\partial\alpha_2} + \frac{\partial h_1}{\partial\alpha_2}\tau_{12} - \frac{\partial h_2}{\partial\alpha_1}\tau_{22}\right] \\ &+ \frac{\mathbf{e}_2}{h_1 h_2}\left[-\frac{\partial h_1}{\partial\alpha_2}\tau_{11} + \frac{\partial(h_2\tau_{12})}{\partial\alpha_1} + \frac{\partial h_2}{\partial\alpha_1}\tau_{21} + \frac{\partial(h_1\tau_{22})}{\partial\alpha_2}\right]\end{aligned} \tag{3}$$

where α_1 and α_2 denote the two parameters defining the interface such that $\alpha_1 =$ constant and $\alpha_2 =$ constant give two sets of mutually orthogonal curves on Γ, and h_1 and h_2 are the corresponding metric coefficients. R_1 and R_2 are the radii of the principal curvatures, and τ_{11}, τ_{22} and τ_{12} are the components of the interface stress tensor $\boldsymbol{\tau}$. As can be seen from equation (3), the first term on the right hand side corresponds to the classical Young-Laplace equation; the remaining terms signify that a non-uniform distribution of the interface stress or a uniform interface stress on a surface with varying curvature needs to be balanced by a bulk shear stress in the abutting materials.

Besides the generalized Young-Laplace equation (2), we need interface constitutive equation to solve a boundary-value problem with the interface stress effect. For an elastically isotropic surface/interface, these are [11]

$$\boldsymbol{\tau} = 2\mu_s\boldsymbol{\varepsilon}_s + \lambda_s(\mathrm{tr}\boldsymbol{\varepsilon}_s)\mathbf{1} \tag{4}$$

where λ_s and μ_s are the surface/interface elastic moduli, and $\mathbf{1}$ is the second-order unit tensor in a two-dimensional space.

2.2. Eshelby formalism. The Eshelby tensors [13,14] for inclusions/inhomogeneities are fundamental to the solution of many problems in materials science, solid state physics and mechanics of composites. Here, we present the tensors for the spherical inhomogeneity problem with the interface stress effect. If an *inhomogeneous inclusion*, i.e. an inhomogeneity embedded in an alien infinite medium is given a uniform eigenstrain, the Eshelby tensors $\mathbf{S}^k(\mathbf{x})$ $(k = I, m)$ relate the total strains $\boldsymbol{\varepsilon}^k(\mathbf{x})$ in the inhomogeneity $(k = I)$, denoted by Ω_I, and the matrix $(k = m)$, denoted by Ω_m, to the prescribed uniform eigenstrain $\boldsymbol{\varepsilon}^*$ in the inhomogeneity

$$\boldsymbol{\varepsilon}^k(\mathbf{x}) = \mathbf{S}^k(\mathbf{x}) : \boldsymbol{\varepsilon}^* \quad (k = I, m), \quad \forall \mathbf{x} \in \Omega_I + \Omega_m \tag{5}$$

where $\mathbf{x}$ is the position vector. On the other hand, the *interior* and *exterior* stress concentration tensors $\mathbf{T}^k(\mathbf{x})$ $(k = I, m)$ relate the total stresses $\boldsymbol{\sigma}^k(\mathbf{x})$ in the two phases to the prescribed uniform remote stress $\boldsymbol{\sigma}^0$

$$\boldsymbol{\sigma}^k(\mathbf{x}) = \mathbf{T}^k(\mathbf{x}) : \boldsymbol{\sigma}^0 \quad (k = I, m), \quad \forall \mathbf{x} \in \Omega_I + \Omega_m. \tag{6}$$

The Eshelby and stress concentration tensors in the two phases are transversely isotropic with any of the radii being an axis of symmetry. However, it should be noted that unlike the classical counterparts for an ellipsoidal inhomogeneity without the interface stress, the interior Eshelby and stress concentration tensors with the interface stress are generally position-dependent. In the Walpole notation [15] for transversely isotropic tensors, the Eshelby tensor $\mathbf{S}^k(\mathbf{r})$ can be expressed as [7]

$$\mathbf{S}^k(\mathbf{r}) = \widetilde{\mathbf{S}}^k(r)\cdot\widetilde{\mathbf{E}}^T \tag{7}$$

in which

$$\widetilde{\mathbf{S}}^k(r) = \left[\, S_1^k(r) \;\; S_2^k(r) \;\; S_3^k(r) \;\; S_4^k(r) \;\; S_5^k(r) \;\; S_6^k(r) \,\right] \tag{8}$$

$$\widetilde{\mathbf{E}} = \left[\, \mathbf{E}^1 \quad \mathbf{E}^2 \quad \mathbf{E}^3 \quad \mathbf{E}^4 \quad \mathbf{E}^5 \quad \mathbf{E}^6 \,\right] \tag{9}$$

where $\mathbf{r}(\mathbf{r} = r\mathbf{n})$ is the position vector of the material point at which the Eshelby tensor is being calculated. $\mathbf{n} = n_i\mathbf{e}_i$ is the unit vector along the radius passing through this point, and r is the distance from this point to the origin (the centre of the spherical inhomogeneity). n_i are the direction cosines of $\mathbf{r}$ and $i = 1, 2, 3$ denote $x-$, $y-$ and $z-$directions, respectively. $\mathbf{S}_q^k(r)$ (q=1,2,...,6) are functions of r, and $\mathbf{E}^p$ (p= 1,2,..., 6) are the six elementary tensors introduced by Walpole [15]. The stress concentration tensors for the spherical inhomogeneity with the interface stress effect can be expressed as [7]

$$\mathbf{T}^k(\mathbf{r}) = \widetilde{\mathbf{T}}^k(r)\cdot\widetilde{\mathbf{E}}^T \quad (k = I, m) \tag{10}$$

in which

$$\widetilde{\mathbf{T}}^k(r) = \left[\, T_1^k(r) \;\; T_2^k(r) \;\; T_3^k(r) \;\; T_4^k(r) \;\; T_5^k(r) \;\; T_6^k(r) \,\right]. \tag{11}$$

The detailed procedure for obtaining these formulas and the expressions of $\widetilde{\mathbf{S}}^k(r)$ and $\widetilde{\mathbf{T}}^k(r)$ can be found in the paper of Duan et al. [7].

The Eshelby tensor in the inhomogeneous inclusion (and in the matrix) is size-dependent through the two non-dimensional parameters $\kappa_s^r = l_\kappa/R$ and $\mu_s^r = l_\mu/R$, R is the radius of the inhomogeneous inclusion, and $l_\kappa = \kappa_s/\mu_m$ and $l_\mu = \mu_s/\mu_m$ are two intrinsic lengths scales. It is found that the interior Eshelby tensor is, in general, not uniform for an inhomogeneous inclusion with the interface stress effect; it is a quadratic function of the position coordinates. The solution without the interface stress effect can be obtained by setting $\kappa_s = 0$ and $\mu_s = 0$, or letting $R \to \infty$. The interior Eshelby tensor is constant in this case. Under dilatational eigenstrain $\boldsymbol{\varepsilon}^*{=}\varepsilon^0\mathbf{I}$, the total strain in the inhomogeneous inclusion is given by $\boldsymbol{\varepsilon}^I{=}\varepsilon^0\mathbf{S}^I{:}\mathbf{I}$. It can be verified that $\mathbf{S}^I{:}\mathbf{I}$ is a constant tensor even in the presence of the interface stress effect

and thus the stress field in the inhomogeneous inclusion is uniform, confirming the result of Sharma et al. [16] for a dilatational eigenstrain.

2.3. Application: strain distributions in quantum dots. The behaviour of the electronic devices made of alloyed quantum dots (QDs) or QDs with a multi-shell structure (e.g., $In_xGa_{1-x}As$, $CdTe_xSe_{1-x}$, ZnS/CdSe, CdS/HgS/CdS/HgS/CdS) is strongly affected by their enriched but nonuniform composition. It has been demonstrated that the assessment of the composition profiles and strains is important to both the identification of the dominant growth mechanisms and the modelling of the confining potential of quantum dots [17–21]. In the following, by assuming that the lattice constants or the thermal expansion coefficients of alloyed QDs obey Vegard's law [22], we will analyze the strain distribution in and around the alloyed QDs. Moreover, the critical sizes of dislocation-free QDs will be determined.

To reveal the profound effect of a nonuniform composition on the stress state of a QD, consider, for simplicity, a spherical alloyed QD embedded in an infinite matrix. The analytical method is equally applicable to QDs of other shapes, sizes, and composition profiles. We assume that the nonuniform composition of the QD is spherically symmetric, i.e. it is a function of the radial coordinate r only. Therefore, the misfit eigenstrains $\boldsymbol{\varepsilon}^*(r)$ induced by the mismatch of the lattice constants or thermal expansion coefficients can be expressed as [21]

$$\boldsymbol{\varepsilon}^*(r) = \varepsilon^*_{rr}(r)\mathbf{e}_r \otimes \mathbf{e}_r + \varepsilon^*_{\theta\theta}(r)(\mathbf{e}_\theta \otimes \mathbf{e}_\theta + \mathbf{e}_\varphi \otimes \mathbf{e}_\varphi) \quad (12)$$

where $\mathbf{e}_r$, $\mathbf{e}_\theta$ and $\mathbf{e}_\varphi$ are the *local* unit base vectors in the spherical coordinate system, and $\varepsilon^*_{rr}(r)$ and $\varepsilon^*_{\theta\theta}(r)$ are the misfit strains in the radial and tangential directions, respectively. According to Vegard's law [22], the misfit strains induced by the mismatch in the lattice constants and those by the mismatch in the thermal expansion coefficients are [20], respectively, $\varepsilon^*_{rr}(r) = c_r(r)\varepsilon^*_{m0}$, $\varepsilon^*_{\theta\theta}(r) = c_\theta(r)\varepsilon^*_{m0}$, $\varepsilon^*_{rr}(r) = c_r(r)\varepsilon^*_{tm0}$, $\varepsilon^*_{\theta\theta}(r) = c_\theta(r)\varepsilon^*_{tm0}$ where $\varepsilon^*_{m0}(= (a_{in} - a_{ex})/a_{ex})$ and $\varepsilon^*_{tm0}(= (\alpha_{in} - \alpha_{ex})\Delta T)$ are the misfit strains arising from the different lattice constants and the thermal expansion coefficients between different uniform phases respectively, a_{in}, a_{ex} and α_{in}, α_{ex} are the lattice constants and the thermal expansion coefficients of the interior and exterior phases, respectively, and ΔT is the temperature difference. c_r and c_θ are the fractions of the ingredient at the location r in the radial and tangential directions, respectively. If $c_r \equiv 1$ and $c_\theta \equiv 1$, Eq. (12) reduces to that for a uniform composition.

We assume that the elastic constants of the alloyed QD are uniform, and have the same values as the surrounding isotropic matrix [23]. This is a reasonable assumption because the alloyed semiconductor QDs usually contain compounds (e.g., InAs/GaAs, CdTe/CdSe) with nearly identical elastic constants, and it has been validated by comparing isotropic and anisotropic solutions for semiconductor materials [23]. We begin with the eigendisplacement vector $\mathbf{u}^*$ in the free-standing QD. According to the theory of infinitesimal elasticity, the governing equation to obtain $\mathbf{u}^*$ is

$$C_{ijkl}\left(u^*_{k,lj} - \varepsilon^*_{kl,j}\right) = 0 \quad (13)$$

where the eigenstrains $\varepsilon^*_{ij}(\mathbf{x})$ are given in Eq. (12), and C_{ijkl} is the elastic modulus tensor of QD. When the variations of $c_\theta(r)$ and $c_r(r)$ are known, the only non-vanishing component of the displacement vector $\mathbf{u}^*$, viz. $u^*_r(r)$ can be easily determined by Eqs. (12) and (13).

For the considered alloyed spherical QD, the only non-vanishing equation of compatibility of misfit eigenstrains ε^*_{rr} and $\varepsilon^*_{\theta\theta}$ represented in Eq. (12) reduces to an equation relating the radial and tangential alloy composition profiles

$$r\frac{\partial c_\theta(r)}{\partial r} + c_\theta(r) = c_r(r), \quad (14)$$

Eq. (14) is identically satisfied when the composition is uniform, but it imposes restrictions on c_r and c_θ when the composition is nonuniform. The strain fields induced by nonuniform composition profiles that meet Eq. (14) are vastly different from those induced by profiles that violate this condition, howsoever slightly. Thus, the compatibility condition (Eq. (14)) provides a theoretical basis for designing the composition profile of an alloyed QD and for estimating its lattice deformation.

Without loss of generality, we consider following two cases of linear composition: Case I: compatible composition profile satisfying Eq. (14), e.g., $c_\theta(r) = k_0 + k_1 r/r_{co}$, $c_r(r) = k_0 + 2k_1 r/r_{co}$, where k_0 and k_1 are two constants and r_{co} is the radius of the QD; Case II: composition profile not satisfying Eq. (14), $c_\theta(r) = c_r(r) = k_0 + k_1 r/r_{co}$. The expressions of the elastic strain in the alloyed QD and the uniform matrix due to the misfit eigenstrains for Cases I and II can be found in the papers of Duan et al. [20,21]. It is found that, the strain field in the alloyed QD is uniform irrespective of the composition profile provided the nonuniform misfit eigenstrains satisfy the compatibility equation, but not otherwise.

In the following, we will calculate the critical radius of the spherical alloyed QD at which the nucleation of a misfit prismatic dislocation (MD) loop becomes energetically favourable. We will again study the effect of the compatibility of misfit strains. The condition for the nucleation of an MD loop is $E_L + W_{IL} \leq 0$ [21], where E_L is the elastic energy of the prismatic dislocation loop and W_{IL} is the interaction energy between it and the QD. According to the condition for the nucleation of an MD loop just mentioned, the critical radii R_{cI} (for Case A) and R_{cII} (for Case B) are

$$R_{cI} = \frac{R_{c0}}{(k_0 + k_1)}, \qquad R_{cII} = \frac{R_{c0}}{(k_0 + 0.75k_1)} \quad (15)$$

where R_{c0} is the critical radius of a spherical QD under uniform hydrostatic eigenstrain ε^*_{m0} [21,24]. It can be seen from Eq. (15) that $R_{cI}/R_{cII} = 1 - 0.25k_1/(k_0 + k_1)$. It is evident that, $k_0 > 0$, $k_0 + k_1 > 0$. Generally, for

the "self-capping" alloyed QD (e.g., $In_xGa_{1-x}As$ on GaAs substrate), the core is enriched in In whereas the outermost layer becomes progressively depleted in In [25]. Therefore, in the composition profile chosen here, $k_1 < 0$. The numerical results show that dislocation nucleation is more difficult in a compositionally nonuniform QD than in a uniform one (cf., $R_{cr}/R_{c0} > 1$ in both situations). However, it is even more difficult when the compatibility equation is satisfied than when it is not ($R_{cI}/R_{c0} > R_{cII}/R_{c0}$ for $k_1 < 0$) [21].

3. Micromechanical framework with surface/interface stress effects

3.1. Micromechanical framework. Consider a representative volume element (RVE) consisting of a two-phase medium occupying a volume V with external boundary S, and let V_I and V_m denote the volumes of the two phases Ω_I and Ω_m. The interface stress effect is taken into account at the interface Γ with outward unit normal $\mathbf{n}$ between Ω_I and Ω_m. The composite is assumed to be statistically homogeneous with the inhomogeneity moduli $\mathbf{C}^I$ (compliance tensor $\mathbf{D}^I$) and matrix moduli $\mathbf{C}^m$(compliance tensor $\mathbf{D}^m$). f and $1-f$ denote the volume fractions of the inhomogeneity and matrix, respectively.

Under homogeneous displacement boundary condition $\mathbf{u}(S) = \boldsymbol{\varepsilon}^0 \cdot \mathbf{x}$, define a strain concentration tensor $\mathbf{R}$ in the inhomogeneity and a strain concentration tensor $\mathbf{T}$ at the interface such that [26]

$$\begin{cases} \bar{\boldsymbol{\varepsilon}}^I = \mathbf{R} : \boldsymbol{\varepsilon}^0 \\ \dfrac{1}{V_I}\displaystyle\int_\Gamma ([\boldsymbol{\sigma}] \cdot \mathbf{n}) \otimes \mathbf{x}\, d\Gamma = \mathbf{C}^m : \mathbf{T} : \boldsymbol{\varepsilon}^0. \end{cases} \tag{16}$$

Then the effective stiffness tensor $\bar{\mathbf{C}}$ of the composite is given by

$$\bar{\mathbf{C}} = \mathbf{C}^m + f\left[\mathbf{C}^I - \mathbf{C}^m\right] : \mathbf{R} + f\mathbf{C}^m : \mathbf{T}. \tag{17}$$

Under the homogeneous traction boundary condition $\boldsymbol{\Sigma}(S) = \boldsymbol{\sigma}^0 \cdot \mathbf{N}$, define two stress concentration tensors $\mathbf{U}$ (in the inhomogeneity) and $\mathbf{W}$ (at the interface) by the relations [26]

$$\begin{cases} \bar{\boldsymbol{\sigma}}^I = \mathbf{U} : \boldsymbol{\sigma}^0 \\ \dfrac{1}{V_I}\displaystyle\int_\Gamma ([\boldsymbol{\sigma}] \cdot \mathbf{n}) \otimes \mathbf{x}\, d\Gamma = \mathbf{W} : \boldsymbol{\sigma}^0. \end{cases} \tag{18}$$

Then the effective compliance tensor $\bar{\mathbf{D}}$ of the composite is given by

$$\bar{\mathbf{D}} = \mathbf{D}^m + f\left[\mathbf{D}^I - \mathbf{D}^m\right] : \mathbf{U} - f\mathbf{D}^m : \mathbf{W}. \tag{19}$$

Equations (16) and (19) can be used to calculate the effective moduli of composites by using the dilute concentration approximation and generalized self-consistent method (GSCM) [27], once $\mathbf{R}$, $\mathbf{T}$, $\mathbf{U}$ and $\mathbf{W}$ have been obtained. Duan et al. [26] have also given formulas to be used together with the Mori-Tanaka method (MTM) [28] to calculate the effective moduli. These are not reproduced here.

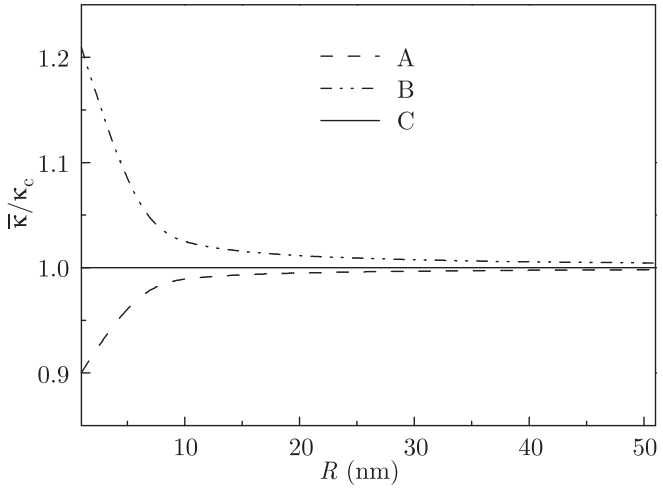

Fig. 1. Effective bulk modulus as a function of void radius ($f = 0.3$)

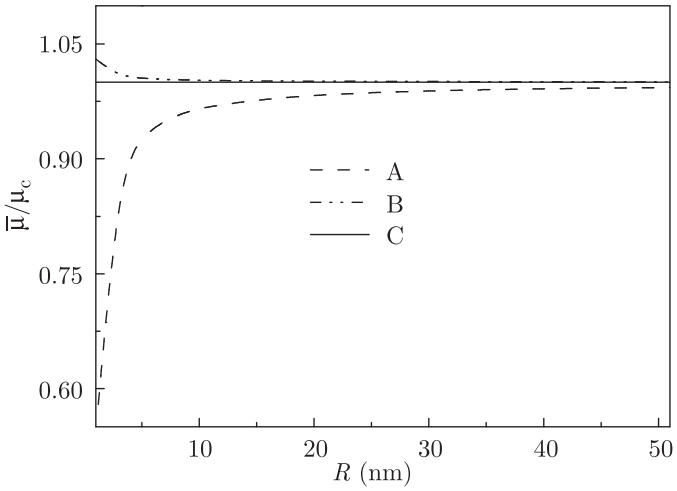

Fig. 2. Effective shear modulus as a function of void radius ($f = 0.3$)

Using the above schemes and the composite spheres assemblage model (CSA) [29], Duan et al.[26] gave detailed expressions for effective bulk and shear moduli of composites containing spherical inhomogeneities with the interface stress effect. They found that, like the classical case without the interface stress effect, the CSA , MTM and GSCM give the same prediction of the effective bulk modulus for a given composite, but unlike the classical results, these effective moduli depend on the size of the inhomogeneities. Like the Eshelby and the stress concentrations tensors in the preceding section, the effective moduli are functions of the two intrinsic length scales $l_\kappa = \kappa_s/\mu_m$ and $l_\mu = \mu_s/\mu_m$. Duan et al. [26] calculated the effective moduli of aluminium containing spherical nano-voids using the free-surface properties obtained by molecular dynamic simulations [4]. Two sets of surface moduli are used, namely, A: $\kappa_s = -5.457$ N/m , $\mu_s = -6.2178$ N/m for surface [1 0 0]; B: $\kappa_s = 12.932$ N/m, $\mu_s = -0.3755$ N/m for surface [1 1 1]. The normalized bulk modulus $\bar{\kappa}/\kappa_c$ for different surface properties as a function of the void radius

R is plotted in Fig. 1, and the variation of $\bar{\mu}/\mu_c$ (calculated by generalized self-consistent method (GSCM)) is plotted in Fig. 2, where "A" and "B" denote the two sets of surface properties, respectively, and "C" the classical result. κ_c and μ_c represent the classical results without the surface effect. It is found that the surface stress effect has a significant effect on the effective bulk and shear moduli, especially when nano-voids are less than 10 nm in radius. The surface stress effect becomes negligible when the radius is larger than 50 nm.

3.2. Elastic moduli of nanochannel-array materials. Nanochannel-array materials have been extensively used in nanotechnology. They can be used as filters and in catalytic convertors, as well as templates for nanosized magnetic, electronic, and optoelectronic devices [2,3,30]. As these materials possess a large surface area, pore surfaces can be modified to create nanoporous materials that are very stiff and light and have very low thermal conductivity. One important immediate application of these materials is as cores in sandwich construction.

Duan et al. [31] have calculated the effective elastic constants of nanochannel-array materials containing randomly or hexagonally distributed but aligned cylindrical pores. Here, we only discuss the effective transverse in-plane modulus k_e and longitudinal shear modulus μ_{Le}.

If the matrix and the surface of the cylindrical pores are both isotropic, k_e is given by [31]

$$k_e = k_m \frac{(1-2\nu_m)\,[2(1-f)+(1+f-2f\nu_m)A]}{2(1+f-2\nu_m)+(1-f)(1-2\nu_m)A} \tag{20}$$

where A=$(\lambda_s+2\mu_s)/(\rho_0\mu_m)$ is a mixed parameter related to the surface elastic properties and the radius ρ_0 of the pores, f is the porosity, and k_m, μ_m and ν_m are the plane-strain bulk modulus, shear modulus and Poisson ratio of the matrix. A becomes vanishingly small when the surface stress effect is negligible, e.g. when the pore radius ρ_0 becomes large. Eq. (20) then gives the effective bulk modulus of a conventional cellular material that is always smaller than k_m. However, it is clear from Eq. (20) that if A exceeds a critical value A_{cr}, the elastic modulus of a nano-cellular material will exceed that of the matrix material! This critical value A_{cr} is independent of the porosity and is simply

$$A_{cr} = \frac{2}{(1-2\nu_m)}. \tag{21}$$

If the Poisson ratio of the non-porous material is say ν_m=0.3, then the critical value A_{cr} is 5, so that the combined surface elastic constant $\lambda_s+2\mu_s=5\rho_0\mu_m$. The variation in the effective transverse bulk modulus in Eq. (20) with the porosity f and the mixed surface parameter A is shown in Fig. 3. The light shaded area represents the region where $k_e/k<1$ and the dark shaded area the region where $k_e/k>1$.

The effective longitudinal shear modulus μ_{Le} of the nano-cellular material, which determines its resistance to shearing along the direction of the pores, is given by [31]

$$\mu_{Le} = \mu_m \frac{[1-f+(1+f)B]}{[1+f+(1-f)B]}. \tag{22}$$

The mixed surface parameter is B=$\mu_s/(\rho_0\mu_m)$. It is easy to see that there also exists a critical value B_{cr}=1 and when $B > B_{cr}$, μ_{Le} of the cellular material will exceed that of the non-porous counterpart. A cellular core with high shear modulus has a great potential in lightweight aerospace construction.

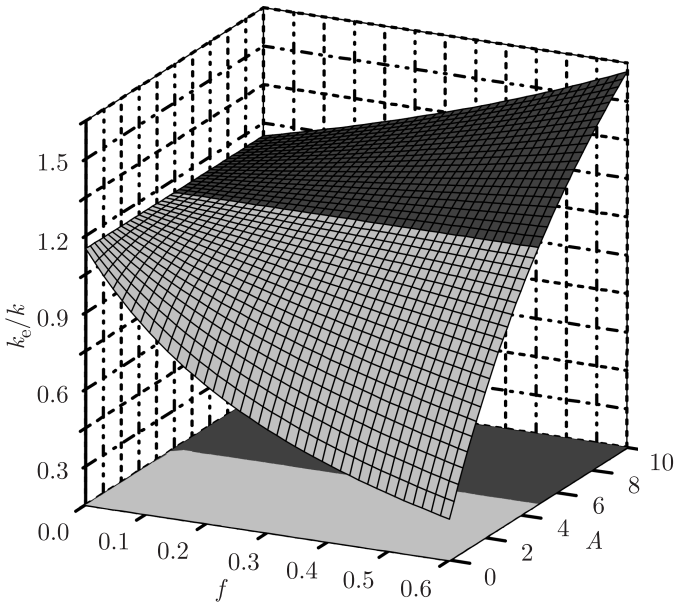

Fig. 3. The normalized effective transverse bulk modulus of a nano-cellular material versus the porosity f and the surface property A

An alternative route to achieving the stiffening of a transversely isotropic nano-cellular material is by coating the cylindrical pore surfaces. Following the procedure in the recent work of Wang et al. [32], it can be proved that the effect of the surface elasticity is equivalent to that of a thin surface layer on the pore surface, i.e.,

$$\lambda_s = \frac{2\mu_I\nu_I\delta}{(1-\nu_I)}, \quad \mu_s = \mu_I\delta. \tag{23}$$

Here, ν_I and μ_I are the Poisson ratio and the shear modulus of the surface coating layer, respectively, and δ is its thickness.

Therefore, by a proper choice of the properties and thickness of a coating layer, materials with cylindrical nanopores can be designed to be stiffer than their non-porous counterparts. For coated cylindrical pores, the effective elastic constants are still given by Eqs. (20) and (22) but with different expressions for the parameters A and B obtained from Eq. (23)

$$A = \frac{2}{(1-\nu_I)}\frac{\delta}{\rho_0}\frac{\mu_I}{\mu}, \quad B = \frac{\delta}{\rho_0}\frac{\mu_I}{\mu}. \tag{24}$$

The critical value A_{cr} for surface stiffening is still given by Eq. (21), and B_{cr} is still equal to 1. If we let $\nu_I = 0.3$,

$\delta = 1$ nm and ρ_0=10 nm, then when the shear modulus ratio μ_I/μ exceeds 17.5, $k_e > k$; when μ_I/μ exceeds 10, $\mu_{Le} > \mu$. From the theoretical analysis mentioned above, it can be seen that the stiffening effect can be easily obtained by surface coating.

The above procedures to increase the stiffness of the nanoporous materials can find applications in many areas of industry. For example, sandwich panels used in many industrial applications contain cellular cores, e.g., honeycombs, with pores aligned perpendicular to the facets [33]. The shear rigidity of such panels and therefore their resistance to shape change are determined by the effective longitudinal shear modulus in Eq. (22) of the cellular cores. Thus, a cellular core with a high shear modulus has great potential in the fabrication of lightweight sandwich structures which are vital for aerospace engineering and other transport industries. Although the microstructures of the nanoporous materials are not exactly the same as those of the conventional honeycombs, the analysis reported above can be regarded as a first step towards increasing the stiffness of porous materials by surface modification.

4. Scaling laws for properties of nano-structured materials

The study of the variation of the properties of materials with their geometrical feature size has a long history because of its importance in many fields [34,35]. Surface/interface stress has a profound effect on the properties of nano-structured and heterogeneous materials due to the large ratio of surface/interface atoms to the bulk. The properties of the nano-structured materials are affected by the energy competition between the surface and bulk, and a common feature of many physical properties is that when the characteristic size of the object is very large, the physical property under consideration tends to that of the bulk material.

For the nano-structured materials, the elasticity of an isotropic surface is characterized by two surface elastic constants λ_s and μ_s [16,36], giving rise to two intrinsic length scales l_λ=λ_s/E and l_μ=μ_s/E [7,26]. It has been shown that the size-dependence of non-dimensional mechanical properties associated with the deformation problems of heterogeneous nano-solids can be expected to follow a scaling law with an intrinsic length scale which is a linear combination of these two scales [37]:

$$\frac{H(L)}{H(\infty)} = 1 + \frac{1}{L}(\alpha_\kappa l_\lambda + \beta_\mu l_\mu). \tag{25}$$

Here, α_κ and β_μ are two non-dimensional parameters, $H(L)$ is the property corresponding to a characteristic size L at nano-scale, and $H(\infty)$ denotes the same property when $L\to\infty$ or, equivalently, when the surface stress effect is vanishingly small. The scaling law (25) is applicable to a wide variety of properties, e.g., the maximum stress concentration factor at the boundary of a circular nano-pore in a plate under uniaxial tension, the effective elastic moduli of the nanochannel-array material, and the Eshelby tensor of a spherical inhomogeneity [37]. For example, the scaling law of the maximum stress concentration factor $k(\rho)$ at the boundary of a circular nano-pore of radius ρ in a plate under uniaxial tension is

$$\frac{k(\rho)}{k(\infty)} = 1 - \frac{7(l_\lambda + 2l_\mu)}{3\rho}. \tag{26}$$

where $k(\infty)$ =3 is the classical elasticity result. We compare the exact results with the scaling law in Eq. (26), and the results are shown in Fig. 4, where "A" and "B" denote the two sets of surface property parameters given in Section 3.1, and the material of the plate is aluminium. It is seen that the scaling law is very accurate.

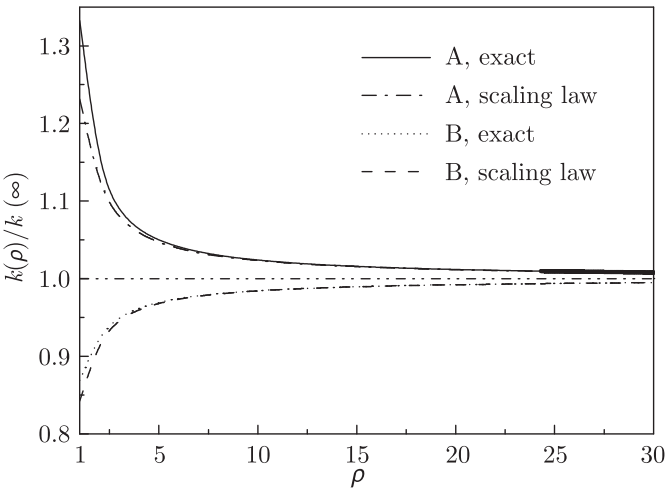

Fig. 4. Comparison of the scaling law and the exact result of the maximum stress concentration factor $k(\rho)/k(\infty)$ at the boundary of a circular nano-pore of radius ρ in a plate (aluminium) under uniaxial tension

As mentioned above, the surface/interface stress has a great effect on the elastic property of nano-structured materials, and this effect can be characterized by the interface stress model (ISM) (Eqs. (2) and (4)), i.e., the displacement is continuous, but the stress is discontinuous across the interface. Apart from the interface stress model, linear spring model (LSM) has been extensively used in simulating the interface property of the heterogeneous materials. In the LSM, it is assumed that the normal and tangential interface displacement discontinuities are each proportional to their associated traction components [37,38,39,40] gave a simple scaling law governing the effective elastic moduli of a two-phase heterogeneous material containing spherical particles or cylindrical fibres with LSM interfaces,

$$\frac{H(\infty)}{H(L)} = 1 + \frac{1}{L}(\alpha_r l_r + \beta_\theta l_\theta) \tag{27}$$

where l_r and l_θ are two intrinsic lengths, and α_r and β_θ are two non-dimensional parameters.

For the thermal conductivity of the heterogeneous materials, there are two extensively used interface models, namely, high conducting (HC) interface model and

low conducting (LC) interface model [41]. It has been demonstrated that the effective thermal conductivity of a two-phase heterogeneous material with HC-type interface can be accurately expressed by a scaling law similar to Eq. (25), and that with LC-type interface by a scaling law similar to Eq. (27) It is interesting to point out that as the interface properties simulated by the two types of interface model (ISM/HC and LSM/LC) have opposite physical interpretations, the corresponding scaling laws, Eqs. (25) and (27) also depict a formal mathematical reciprocity.

5. Conclusions

This paper summarizes the recent results of some fundamental problems in mechanics of heterogeneous materials where the surface/interface stress is taken into account, thus extending the continuum mechanics to the nano-scale. These include the Eshelby tensors, stress concentration tensors and their applications, the micromechanical framework, the novel properties of nanochannel-array materials, and the generalized Levin's formula and Hill's connections. These results show that the surface/interface stress has an important effect on the mechanical properties of materials at the nano-scale. When the surface/interface elasticity is taken into account, some length scales emerge automatically. Thus, unlike their classical counterparts, the mechanical properties at the nano-scale become, as expected, size-dependent. The scaling laws governing the properties of nano-structured materials are given.

Acknowledgements. One of the authors, Duan, is being funded by a Post-doctoral Fellowship from The Royal Society, London.

References

[1] H. Gleiter, "Naostructured materials: basic concepts and microstructure", *Acta Mater.* 48, 1–29 (2000).

[2] H. Masuda and K. Fukuda, "Ordered metal nanohole arrays made by a two-step replication of honeycomb structures of anodic alumina", *Science* 268, 1466–1468 (1995).

[3] C.R. Martin and Z. Siwy, "Molecular filters-pores within pores", *Nature Mater.* 3, 284–285 (2004).

[4] R.E. Miller and V.B. Shenoy, "Size-dependent elastic properties of nanosized structural elements", *Nanotech.* 11, 139–147 (2000).

[5] S. Cuenot, C. Frétigny, S. Demoustier-Champagne, and B. Nysten, "Surface tension effect on the mechanical properties of nanomaterials measured by atomic force microscopy", *Phys. Rev.* B 69, 165410 (2004).

[6] L.G. Zhou and H.C. Huang "Are surfaces elastically softer or stiffer?", *Appl. Phys. Lett.* 84, 1940–1942 (2004).

[7] H.L. Duan, J. Wang, Z.P. Huang, and B.L. Karihaloo, "Eshelby formalism for nano-inhomogeneities", *Proc. Roy. Soc. Lond.* A 461, 3335–3353. (2005).

[8] V.B. Shenoy, "Atomistic calculations of elastic properties of metallic fcc crystal surfaces", *Phys. Rev.* B 71, 094104 (2005).

[9] G.Y. Jing, H.L. Duan, X.M. Sun, Z.S. Zhang, J. Xu, Y.D. Li, J. Wang, and Yu, D.P., "Surface effects on elastic properties of silver nanowires: contact atomic-force microscopy", *Phys. Rev.* B 73, 235409 (2006).

[10] P. Müller and A. Saúl, "Elastic effects on surface physics", *Surf. Sci. Reports* 54, 157–258 (2004).

[11] M.E. Gurtin and A.I. Murdoch, "A continuum theory of elastic material surfaces", *Arch. Rat. Mech. Anal.* 57, 291–323 (1975).

[12] Y.Z. Povstenko, "Theoretical investigation of phenomena caused by heterogeneous surface-tension in solids", *J. Mech. Phys. Solids* 41, 1499-1514 (1993).

[13] J.D. Eshelby, "The determination of the elastic field of an ellipsoidal inclusion and related problems", *Proc. R. Soc. Lond.* A 241, 376–396 (1957).

[14] J.D. Eshelby, "The elastic field outside an ellipsoidal inclusion", *Proc. R. Soc. Lond.* A 252, 561–569 (1959).

[15] L.J. Walpole, "Elastic behaviour of composite materials: theoretical foundations", *Advances in Appl. Mech.* 21, 169–242 (1981).

[16] P. Sharma, S. Ganti, and N. Bhate, "Effect of surfaces on the size-dependent elastic state of nano-inhomogeneities", A*ppl. Phys. Lett.* 82, 535–537 (2003).

[17] D. Rosenauer and D. Gerthsen, "Atomic scale strain and composition evaluation from high-resolution transmission electron microscopy images", *Advances in Imaging and Electron Physics* 107, 121–130 (1999).

[18] A. Malachias, S. Kycia, G. Medeiros-Ribeiro, R. Magalhaes-Paniago, T.I. Kamins, and R.S. Williams, "3D composition of epitaxial nanocrystals by anomalous x-ray diffraction: Observation of a Si-rich core in Ge domes on Si(100)", *Phys. Rev. Lett.* 91, 176101 (2003).

[19] B.J. Spencer and M. Blanariu, "Shape and composition map of a prepyramid quantum dot", *Phys. Rev. Lett.* 95, 206101 (2005).

[20] H.L. Duan, B.L. Karihaloo, J. Wang, and X. Yi, "Strain distributions in nano-onions with uniform and non-uniform compositions", *Nanotech.* 17, 3380–3387 (2006).

[21] H.L. Duan, B.L. Karihaloo, J. Wang, and X. Yi, "Compatible composition profiles and critical sizes of alloyed quantum dots", *Phys. Rev.* B 74, 195328 (2006).

[22] L. Vegard, "The constitution of mixed crystals and the space occupied by atoms", *Z. Phys.* 5, 17–26 (1921).

[23] D.A. Faux and G.S. Pearson, "Green's tensors for anisotropic elasticity: application to quantum dots", *Phys. Rev.* B 62, R4798–4801 (2000).

[24] A.L. Kolesnikova and A.E. Romanov, "Misfit dislocation loops and critical parameters of quantum dots and wires", *Phil. Mag. Lett.* 84, 501–506 (2004).

[25] J. Tersoff, "Enhanced nucleation and enrichment of strained-alloy quantum dots", *Phys. Rev. Lett.* 81, 3183–3186 (1998).

[26] H.L. Duan, J. Wang, Z.P. Huang, and B.L. Karihaloo, "Size-dependent effective elastic constants of solids containing nano-inhomogeneities with interface stress", *J. Mech. Phys. Solids* 53, 1574–1596 (2005).

[27] R.M. Christensen and K.H. Lo, "Solutions for effective shear properties in three phase sphere and cylinder models", *J. Mech. Phys. Solids* 27, 315–330 (1979).

[28] T. Mori and K. Tanaka, "Average stress in matrix and average elastic energy of materials with misfitting inclusions", *Acta Metall.* 21, 571–574 (1973).

[29] Z. Hashin, "The elastic moduli of heterogeneous materials", *J. Appl. Mech.* 29, 143–150 (1962).

[30] J.L. Shi, Z.L. Hua, and L.X. Zhang, "Nanocomposites from ordered mesoporous materials", *J. Mater. Chem.* 14, 795–806 (2004).

[31] H.L. Duan, J. Wang, B.L. Karihaloo, and Z.P. Huang, "Nanoporous materials can be made stiffer than nonporous counterparts by surface modification", *Acta Mater.* 54, 2983–2990 (2006).

[32] J.Wang, H.L. Duan, Z. Zhang, and Z.P. Huang, "An anti-interpenetration model and connections between interphase and interface models in particle-reinforced composites", *Int. J. Mech. Sci.* 47, 701–718 (2005).

[33] L.J. Gibson and M.F. Ashby, *Cellular Solids – Structure and Properties*, 2nd ed., Cambridge Univ. Press, Cambridge, 1997.

[34] K. Kendall, "Impossibility of comminuting small particles by compression", *Nature* 272, 710–711 (1978).

[35] B.L. Karihaloo, "Impossibility of comminuting small particles by compression", *Nature* 279, 169–170 (1979).

[36] D.J. Bottomley and T. Ogino, "Alternative to the Shuttleworth formulation of solid surface stress", *Phys. Rev.* B 63, 165412 (2001).

[37] J. Wang, H.L. Duan, Z.P. Huang, and B.L. Karihaloo, "A scaling law for properties of nano-structured materials", *Proc. Roy. Soc. Lond.* A 462, 1355–1363 (2006).

[38] Z. Hashin, "Thermoelastic properties of particulate composites with imperfect interface", *J. Mech. Phys. Solids* 39, 745–762 (1991).

[39] Y. Benveniste and T. Miloh, "Imperfect soft and stiff interfaces in two-dimensional elasticity", *Mech. Mater.* 33, 309–323 (2001).

[40] H.L. Duan, X. Yi, Z.P. Huang, and J. Wang, "A unified scheme for prediction of effective moduli of multiphase composites with interface effects: Part II – application and scaling laws", *Mech. Mater.* 39, 94–103 (2007).

[41] T. Miloh and Y. Benveniste, "On the effective conductivity of composites with ellipsoidal inhomogeneities and highly conducting interfaces", *Proc. R. Soc. Lond.* A 455, 2687–2706 (1999).